Metallomics

PAPER

View Article Online
View Journal | View Issue

Cite this: *Metallomics*, 2017, 9, 556

Tight binding of heme to *Staphylococcus aureus* IsdG and IsdI precludes design of a competitive inhibitor†

Matthew A. Conger, Deepika Pokhrel and Matthew D. Liptak *

The micromolar equilibrium constants for heme dissociation from IsdG and IsdI reported in the literature call into question whether these enzymes are actually members of the iron-regulated surface determinant system of *Staphylococcus aureus*, which harvests heme iron from a host during infection. In order to address this question, the heme dissociation constants for IsdG and IsdI were reevaluated using three approaches. The heme dissociation equilibrium constants were measured using a UV/Vis absorption-detected assay analyzed with an assumption-free model, and using a newly developed fluorescence-detected assay. The heme dissociation rate constants were estimated using apomyoglobin competition assays. Analyses of the UV/Vis absorption data revealed a critical flaw in the previous measurements; heme is 99.9% protein-bound at the micromolar concentrations needed for UV/Vis absorption spectroscopy, which renders accurate equilibrium constant measurement nearly impossible. However, fluorescence can be measured for more dilute samples, and analyses of these data resulted in dissociation equilibrium constants of 1.4 ± 0.6 nM and 12.9 ± 1.3 nM for IsdG and IsdI, respectively. Analyses of the kinetic data obtained from apomyoglobin competition assays estimated heme dissociation rate constants of 0.022 ± 0.002 s^{-1} for IsdG and 0.092 ± 0.008 s^{-1} for IsdI. Based upon these data, and what is known regarding the post-translational regulation of IsdG and IsdI, it is proposed that only IsdG is a member of the heme iron acquisition pathway and IsdI regulates heme homeostasis. Furthermore, the nanomolar dissociation constants mean that heme is bound tightly by IsdG and indicates that competitive inhibition of this protein will be difficult. Instead, uncompetitive inhibition based upon a detailed understanding of enzyme mechanism is a more promising antibiotic development strategy.

Received 10th February 2017,
Accepted 4th April 2017

DOI: 10.1039/c7mt00035a

rsc.li/metallomics

Significance to metallomics

Staphylococcus aureus uses the iron-regulated surface determinant system to acquire an essential nutrient, iron, from its host organism. Here, the heme dissociation constants for two putative members of this pathway have been measured. These data provide insight into heme iron trafficking and homeostasis in *S. aureus*.

Introduction

Staphylococcus aureus is a Gram-positive human pathogen that has been labelled a serious antibiotic-resistant threat by the Centers for Disease Control and Prevention. The major concern is the growing number of methicillin- and even vancomycin-resistant cases,[1] which means that humans are in a race against *S. aureus* to develop a new antibiotic before all known drugs become ineffective. A promising target is the iron-regulated surface determinant (Isd) system of *S. aureus*,[2] which is responsible for harvesting an essential nutrient, iron, from a mammalian host during infection.[3] The Isd system consists of nine proteins that: bind host hemoglobin, extract the heme cofactor, import heme into the bacterial cytosol,[4] and degrade heme to iron,[5] staphylobilin,[6] and formaldehyde.[7] The final two enzymes of this pathway responsible for heme degradation, IsdG and IsdI, appear to be potentially promising antibiotic targets since their inhibition would not only starve *S. aureus* of a vital nutrient, iron,[3] but also lead to the build-up of a toxic molecule, heme.[8] Indeed, it has been shown that both IsdG and

Department of Chemistry, University of Vermont, Burlington, Vermont 05405, USA. E-mail: matthew.liptak@uvm.edu

† Electronic supplementary information (ESI) available: Derivations of eqn (1) and (2), SDS-PAGE gels, UV/Vis absorption spectra for apomyoglobin competition assays, complete fit of fluorescence-detected titration of heme into IsdI, fits of 340 nm emission data. See DOI: 10.1039/c7mt00035a

IsdI are required for pathogenesis in mice.[3] However, there remain several open questions regarding the biochemistry of IsdG and IsdI that must be answered before a selective inhibitor of these enzymes can be designed.

The fundamental issue is that IsdG and IsdI have similar enzymatic functions to human heme oxygenases (HOs), and the differences between the enzyme families must be elucidated in order to selectively inhibit IsdG and IsdI in the presence of human HOs. Human HOs are members of a class of enzymes known as canonical HOs that oxygenate heme to biliverdin,[9] while IsdG and IsdI are non-canonical HOs that degrade heme to staphylobilin.[6] One difference between these classes of enzymes to potentially target is the first oxygenation reaction catalyzed by both HO families: the conversion of heme to *meso*-hydroxyheme.[10,11] Canonical HOs rely upon a conserved water cluster to guide a transient hydroxyl radical to the *meso* carbon of heme (Fig. 1),[12–14] whereas it has been proposed that non-canonical HOs proceed through a bridged Fe–O–O–C transition state.[15,16] Another target for selective inhibition of IsdG and IsdI in the presence of human HOs is the *meso*-hydroxyheme intermediate. In canonical HOs, *meso*-hydroxyheme is converted to verdoheme and biliverdin,[17] whereas IsdG and IsdI convert this intermediate to formyl-oxo-bilin and staphylobilin (Fig. 2).[11] Based upon data available prior to this publication, the most promising strategy for selective inhibition of IsdG and IsdI in the presence of human HOs was competitive inhibition since the dissociation equilibrium constants for heme from IsdG and IsdI were reported to be 1000-fold greater than for heme from human HOs.[5,18,19]

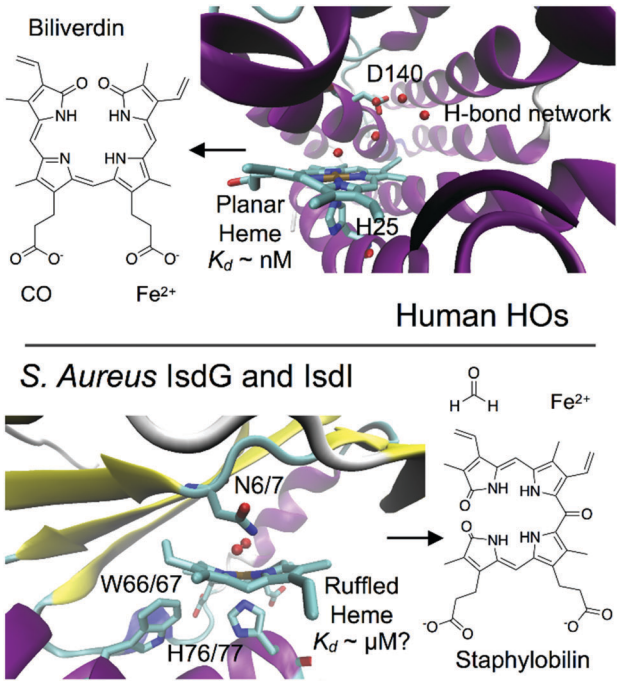

Fig. 1 There are several important differences between human HOs and the non-canonical HOs IsdG and IsdI from *S. aureus*. Human HOs bind heme *via* His25 with nanomolar K_d values and degrade this substrate to biliverdin, carbon monoxide, and iron. Asp140 organizes a network of water molecules that guides a transient hydroxyl radical to the *meso* carbon of heme. In contrast, *S. aureus* IsdG and IsdI have been reported to bind heme *via* His76/77 with micromolar K_d values and produce staphylobilin, formaldehyde, and iron. The second-sphere residues Asn6/7 and Trp66/67 are essential for enzymatic turnover.

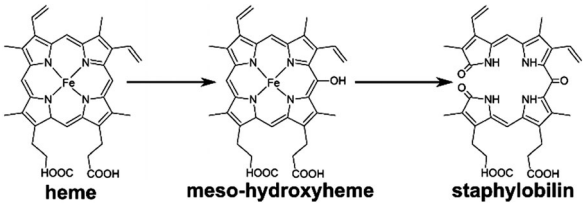

Fig. 2 IsdG and IsdI degrade heme to staphylobilin *via* a *meso*-hydroxyheme intermediate. The first oxygenation reaction proceeds *via* a mechanism that is distinct from that of human HOs. The second oxygenation reaction is unique to IsdG and IsdI.

Nevertheless, several observations call into question the accuracy of the equilibrium dissociation constant (K_d) values reported in the literature for heme-bound IsdG (IsdG–heme) and IsdI (IsdI–heme). First, it was recently reported that the concentration of the cytosolic labile heme pool is 20–40 nM,[20,21] which means that only 1% of cytosolic heme would be bound to IsdG and IsdI under typical conditions based upon the reported micromolar K_d values.[5] It is unrealistic to suggest that the Isd pathway increases the concentration of cytosolic heme to micromolar concentrations, since a recent study has demonstrated that this concentration of heme is toxic to *S. aureus*.[8] Finally, micromolar K_d values for IsdG–heme and IsdI–heme simply do not fit with the observation of this laboratory that heme is almost fully protein-bound following separation of a mixture of IsdG–heme (or IsdI–heme) and heme by size-exclusion chromatography. A potential explanation for these observations relates to the fact that the K_d values for IsdG–heme and IsdI–heme were determined by fitting UV/Vis absorption titration data to a Michaelis–Menten model.[5] Subsequent research has called into question whether this enzyme follows Michaelis–Menten kinetics due to the requirement of at least three substrates,[5,7,11] plus a reductase,[22] and the presence of at least two enzymatic intermediates.[11] Thus, the dissociation constants for IsdG–heme and IsdI–heme were re-investigated.

This paper reports K_d measurements for heme dissociation from *S. aureus* IsdG and IsdI by UV/Vis absorption and fluorescence spectroscopies, and k_{off} estimates from apomyoglobin competition assays. UV/Vis absorption-detected titrations of heme into IsdG and IsdI were fit to a model that did not employ the weak binding approximation, where the total ligand concentration is used to approximate the unbound ligand concentration, resulting in a quadratic equation.[23] This approximation-free model is essential whenever the K_d for ligand dissociation is significantly smaller than the protein concentration. Careful analyses of these data revealed that the values measured by UV/Vis absorption spectroscopy only represent an upper-bound. Thus, a more sensitive fluorescence-detected assay was developed. Fits of the fluorescence-detected titrations yielded accurate K_d values for IsdG–heme and IsdI–heme in the nanomolar range. Analyses of the apomyoglobin

competition assays yielded k_{off} rates on the order of 10^{-2} s^{-1}. The implications of these results for the accuracy of K_d values reported in the literature, for the *in vivo* functions of IsdG and IsdI, and for the design of a selective IsdG inhibitor are discussed.

Experimental

Unless otherwise noted, all materials in this work were purchased from Fisher Scientific and used without further purification.

Expression and purification

The cloning of IsdG and IsdI into pET-15b (Amp^r, Novagen) and S219V tobacco etch virus (TEV) protease into pRK793 (Amp^r) has been previously described.[15,24,25] IsdG and IsdI were expressed as previously described for IsdG,[5] with one change. Expression was induced at OD_{600} = 0.8 with 1.0 mM isopropyl β-D-1-thiogalactopyranoside, and cell growth continued for four hours at 37 °C. S219V TEV protease was expressed and purified as previously described.[15]

IsdG was purified as previously described,[15] with minor changes noted below. Following cleavage of IsdG by S219V TEV protease, 50 mM imidazole was added and the solution was loaded onto a HisPur Ni-NTA column (Pierce). The flow-through was collected and the column was washed with 50 mM Tris pH 7.4, 150 mM NaCl, 50 mM imidazole. The wash was collected and pooled with the flow-through. IsdG was then dialyzed against 1 L of 50 mM Tris pH 7.4, 150 mM NaCl. This procedure yields untagged IsdG in >99% purity as determined by SDS-PAGE gel electrophoresis (Fig. S1, ESI†).

IsdI was purified as previously described,[24] with the following changes. S219V TEV protease was added to His_6-tagged IsdI in an OD_{280} ratio of 1 : 10 with sufficient dithiothreitol and ethylenediaminetetracetic acid to reach final concentrations of 1 mM and 0.5 mM, respectively. The mixture was dialyzed twice against 50 mM NaP_i pH 7.4, 150 mM NaCl; then once against 50 mM Tris pH 7.4, 150 mM NaCl, all at 4 °C. The dialyzed solution was then loaded onto a Ni-NTA column equilibrated with 50 mM Tris pH 7.4, 150 mM NaCl and all flow-through was collected. The flow-through was reloaded onto a Ni-NTA column equilibrated with 50 mM Tris pH 7.4, 150 mM NaCl one additional time and all flow-through was collected. This procedure yields untagged IsdI in >99% purity as determined by SDS-PAGE gel electrophoresis (Fig. S2, ESI†).

Apomyoglobin was prepared *via* extraction of heme from equine skeletal muscle myoglobin (Sigma-Aldrich) using the methyl ethyl ketone method,[26] as recently described.[27]

Spectroscopic characterization

The extinction coefficients for IsdG–heme and IsdI–heme were determined using a procedure similar to one previously described.[15] IsdG–heme and IsdI–heme in 50 mM Tris pH 7.4, 150 mM NaCl were prepared, and their room temperature UV/Vis absorption spectra were acquired from 700 to 325 nm at a scan rate of 600 nm min^{-1} with a 1.0 nm data interval and 0.1 s integration time on a Cary 100 Bio UV-Vis Spectrophotometer. The extinction coefficients for IsdG–heme and IsdI–heme at 411 nm were found to be 98.5 mM^{-1} cm^{-1} and 96.6 mM^{-1} cm^{-1}, respectively, as determined by the pyridine hemochrome method.[28]

UV/Vis absorption-detected heme titrations into IsdG and IsdI were carried out using the same spectroscopic equipment and parameters as described above. 6 μM samples of IsdG and IsdI in 50 mM Tris pH 7.4, 150 mM NaCl were prepared. The protein concentrations were estimated using a Bradford assay. A 250 μM hemin solution was prepared as previously described.[29] Hemin was then titrated into the IsdG and IsdI solution in 1 μM increments. Prior to UV/Vis absorption spectral characterization, the solutions were allowed to equilibrate until no further spectral changes were observed.

Fluorescence-detected heme titrations into IsdG and IsdI were completed using similar protein samples. 60–80 nM samples of IsdG and IsdI, and 17.5 μM hemin solutions, were prepared in 50 mM Tris pH 7.4, 150 mM NaCl as previously described.[29] Hemin was titrated into the IsdG and IsdI solutions in 16 nM increments, and allowed to equilibrate until no further spectral changes were observed. Titrations were considered complete when the fluorescence emission intensity change due to substrate binding was less than one percent of that of substrate-free protein. Fluorescence emission spectra were acquired for 285 nm excitation using a Photon Technology International QuantaMaster 4 spectrofluorometer equipped with a Xenon arc lamp connected to an LPS-220B power supply, an ASOC-10 electronics interface, an MD-4000 motor driver control, and a model 814 photomultiplier detection system. Emission spectra were acquired in the 420 to 300 nm range with a step size of 1 nm, an integration time of 1 s, and slit widths of 3 nm.

For heme dissociation rate measurements, mixtures of 3 μM IsdG–heme and 3 μM IsdG were prepared as described above. These solutions were transferred to Spectrosil quartz cuvettes (Starna) and apomyoglobin, prepared as described above, was added to a final concentration of 30 μM. Following a 7.5 s mixing time, the UV/Vis absorption intensity at 408 nm was monitored as a function of time using the spectroscopic equipment described above with a cycle time of 1.0 s and an integration time of 1.0 s for 30 min. UV/Vis absorption spectra were acquired before and after each kinetics experiment to confirm complete transfer of heme from IsdG to apomyoglobin (Fig. S3, ESI†).[30] Similar experiments were performed for IsdI.

Spectral analysis

The UV/Vis absorption-detected heme titrations into IsdG and IsdI were analysed in order to determine the K_d of the heme substrate. The UV/Vis absorption intensity at 411 nm for a mixture of IsdG, IsdG–heme, and heme depends upon eqn (1):

$$A_{411} = \frac{([\mathrm{IsdG_T}] + [\mathrm{heme_T}] + K_d) - \sqrt{([\mathrm{IsdG_T}] + [\mathrm{heme_T}] + K_d)^2 - 4[\mathrm{IsdG_T}][\mathrm{heme_T}]}}{2} \times (\varepsilon_{\mathrm{IsdG-heme}} - \varepsilon_{\mathrm{heme}}) + \varepsilon_{\mathrm{heme}}[\mathrm{heme_T}] \quad (1)$$

where [IsdG$_T$] is the total IsdG concentration, [heme$_T$] is the total heme concentration, $\varepsilon_{IsdG-heme}$ is the molar extinction coefficient for IsdG–heme at 411 nm, and ε_{heme} is the molar extinction coefficient for heme at 411 nm. The molar extinction coefficient for heme at 411 nm was determined to be 28.3 mM^{-1} cm^{-1} based upon the reported extinction coefficient at 385 nm (58.4 mM^{-1} cm^{-1}).[31] The UV/Vis absorption intensity at 411 nm as a function of [heme$_T$] was fit to eqn (1) using GraphPad Prism 6.0g in order to determine [IsdG$_T$], K_d, and their standard errors. The fitted value for [IsdG$_T$] was compared to the value estimated from a Bradford assay to further assess the accuracy of the fit. A similar equation can be derived for IsdI. The complete derivation of eqn (1) is available in the ESI.†

The heme binding induced quenching of tryptophan fluorescence was analysed to extract K_d for IsdG–heme and IsdI–heme. The tryptophan fluorescence intensity for a mixture of IsdG, IsdG–heme, and heme depends upon eqn (2):

$$F = \frac{([IsdG_T]+[heme_T]+K_d) - \sqrt{([IsdG_T]+[heme_T]+K_d)^2 - 4[IsdG_T][heme_T]}}{2} \times \left(\frac{F_{min}-F_{max}}{[IsdG_T]}\right) + F_{max} \quad (2)$$

where F_{max} is the fluorescence intensity in the absence of heme and F_{min} is the emission intensity for fully heme-bound IsdG. The fluorescence emission intensity at 323 nm as a function of [heme$_T$] was fit to eqn (2) using GraphPad Prism 6.0g to extract K_d and its standard error. [IsdG$_T$] was constrained to the values determined by the UV/Vis absorption titrations described above prior to sample dilution. A similar equation can be derived for 318 nm fluorescence emission from IsdI. The complete derivation of eqn (2) is available in the ESI.†

The first-order rate constants for heme transfer from IsdG–heme or IsdI–heme to apomyoglobin were estimated from the kinetic assays by fitting the UV/Vis absorption intensity at 408 nm to eqn (3):

$$A = A_0 + A_\infty(1 - e^{-k_{off}t}) \quad (3)$$

where A_0 is the UV/Vis absorption intensity at 0 s, A_∞ is the UV/Vis absorption intensity at equilibrium, and k_{off} is the dissociation rate constant. The UV/Vis absorption intensity at 408 nm as a function of time was fit to eqn (3) using Graph Pad Prism 6.0g in order to determine A_0, A_∞, k_{off}, and their standard errors. The fitted values for A_0 and A_∞ were compared to the UV/Vis absorption intensity at 408 nm before and after the kinetic assay to further assess the accuracy of the fit.

Results

UV/Vis absorption spectroscopy

One possible explanation for the discrepancy between the concentration of the labile heme pool and the K_d values for IsdG–heme and IsdI–heme is that the reported K_d values are too large.[5,20,21] This explanation is reasonable because the K_d values reported in the literature were derived from fits of UV/Vis absorption titration data to a Michaelis–Menten kinetic model,[5] and subsequent research has established that IsdG-catalyzed heme degradation does not follow this mechanism.[11] Therefore, UV/Vis absorption-detected titrations of heme into IsdG and IsdI were analysed with an approximation-free model in order to estimate K_d values (Fig. 3). The UV/Vis absorption intensity at 411 nm was monitored as a function of titrated heme concentration since this wavelength corresponds to the intense Soret bands of IsdG–heme and IsdI–heme. These data were fit to eqn (1), which yielded K_d values of 34 ± 20 nM and 15 ± 10 nM for IsdG and IsdI, respectively. These values are two orders of magnitude lower than those previously reported in the literature.[5] At that point, it was clear that the K_d values reported in the literature were inconsistent with those reported here, but it was unclear which data set was more reliable.

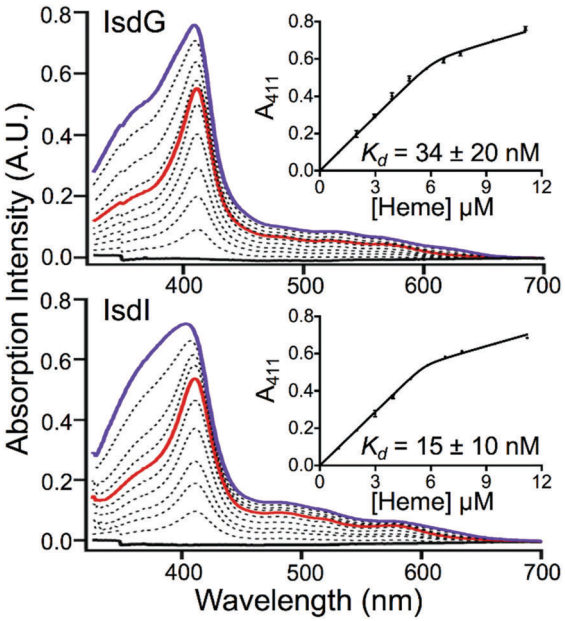

Fig. 3 UV/Vis absorption-detected titration of heme into 6 μM IsdG (top) and IsdI (bottom) in 50 mM Tris pH 7.4, 150 mM NaCl. The spectra depict protein in the presence of 0 (solid black), 1 (solid red), 2 (solid violet), and intermediate (dashed black) equivalents of heme. Fits of the UV/Vis absorption intensity at 411 nm to eqn (1) are shown in the insets, yielding K_d values of 34 ± 20 nM for IsdG and 15 ± 10 nM for IsdI. The vertical error bars represent the standard deviation of at least three independent measurements.

The accuracy of the K_d values measured here by fitting UV/Vis absorption data to an approximation-free binding model was assessed by comparing the experimental data to titration curves predicted for K_d values one order of magnitude smaller and larger than the best fit (Fig. 4). Fits of the IsdG and IsdI data to titration curves for the K_d values one order of magnitude less than the best fit decreased the R^2 values by 0.001 or less. Fits of the titration curves to K_d values one order of magnitude larger than the best fit decreased the R^2 values by approximately 0.01. Therefore, the K_d values reported here based upon UV/Vis absorption analysis are upper limits on the actual K_d values. Based upon the estimated K_d values, nearly all titrated heme is protein-bound for heme : protein ratios up to 1 : 1 at micromolar

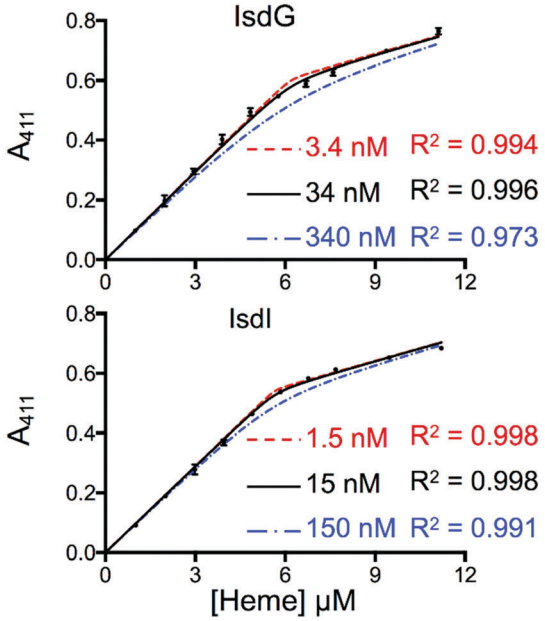

Fig. 4 Best fits of the UV/Vis absorption-detected heme titration data for IsdG (top) and IsdI (bottom) using eqn (1) (solid black). The vertical error bars represent the standard deviation of at least three independent measurements. Titration curves predicted using eqn (1) for K_d values one order of magnitude smaller (dotted red) and larger (dashed blue) than the best fit. Based upon the good fit of the UV/Vis absorption-detected heme titration data to a K_d value one order of magnitude smaller than the best fit, the K_d values estimated by UV/Vis absorption appear to be upper bounds on the actual value.

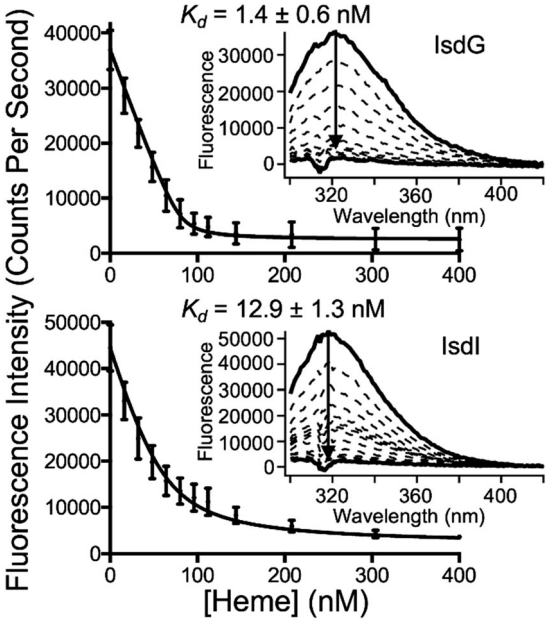

Fig. 5 Fluorescence-detected titration of heme into 80 nM IsdG (top) and 60 nM IsdI (bottom) in 50 mM Tris pH 7.4, 150 mM NaCl. The vertical error bars represent the standard deviation of at least three independent measurements. The emission spectra for 285 nm excitation are shown in the insets. Fits of the emission intensity to eqn (2) yielded K_d values of 1.4 ± 0.6 nM for IsdG and 12.9 ± 1.3 nM for IsdI.

protein concentrations, which greatly limits the accuracy of the measurement. Thus, both the K_d values previously reported in the literature,[5] and those estimated here based upon UV/Vis absorption data, are likely too large due to a fundamental issue with the sensitivity of UV/Vis absorption spectroscopy. Consequently, a more sensitive method for measuring the K_d of heme binding to IsdG and IsdI was sought.

Fluorescence spectroscopy

The greater sensitivity of fluorescence spectroscopy as compared to UV/Vis absorption spectroscopy enabled monitoring of heme binding to IsdG and IsdI at nanomolar concentrations of protein, which increased the concentration of unbound heme and was expected to improve the accuracy of the K_d measurement. The experiments described below rely upon the fact that both IsdG and IsdI have fluorescent Trp residues within 4 Å of the heme substrate,[32] which acts as a quencher *via* Förster resonance energy transfer due to its partially filled Fe 3d subshell. The Trp emission intensity was monitored as a function of titrated heme concentration for 80 nM and 60 nM samples of IsdG and IsdI, respectively (Fig. 5). The fluorescence-detected heme titrations were fit to eqn (2), which gave K_d values of 1.4 ± 0.6 nM for IsdG and 12.9 ± 1.3 nM for IsdI. Due to the higher K_d value for heme from IsdI, the titration into IsdI was continued out to 976 nM heme (Fig. S4, ESI†), but only the data up to 400 nM heme is shown here to ease comparison with IsdG. The fluorescence intensities at 340 nm were also analysed using eqn (2) to avoid the signal arising from the Raman scattering of water, and similar results were obtained (Fig. S5, ESI†). The K_d values derived from fitting fluorescence data are smaller than those estimated from UV/Vis absorption-detected heme titrations reported both here (Fig. 3), and in the literature.[5] Due to the differences between the K_d values derived from UV/Vis absorption and fluorescence-monitored heme titrations, the accuracies of the fluorescence fits were assessed carefully.

As was the strategy for assessing the accuracy of the UV/Vis absorption data, the fluorescence data was compared to titration curves predicted for K_d values one order of magnitude smaller and larger than the best fit (Fig. 6). Fits of the fluorescence data to K_d values one order of magnitude less than the best fit decreased the R^2 values by 0.01 to 0.1. Fits of the IsdG and IsdI data to titration curves for K_d values one order of magnitude larger than the best fit decreased R^2 by approximately 0.1. Thus, the K_d values derived from analysis of the fluorescence data are accurate, and values estimated based upon UV/Vis absorption spectroscopy overestimate K_d for IsdG–heme and IsdI–heme. Importantly, the accurate K_d values measured using fluorescence spectroscopy are consistent with the concentration of the labile heme pool and both enzymes are expected to bind heme tightly *in vivo*.[20,21] It is also interesting to note that the K_d values for IsdG–heme and IsdI–heme are significantly different from one another. In summary, the data presented here indicates that the K_d values for IsdG–heme and IsdI–heme are two to three orders of magnitude lower than previously reported,[5] which is now consistent with the concentration of the labile heme pool,[20,21] and heme binding to IsdG is nine-fold tighter than heme binding to IsdI.

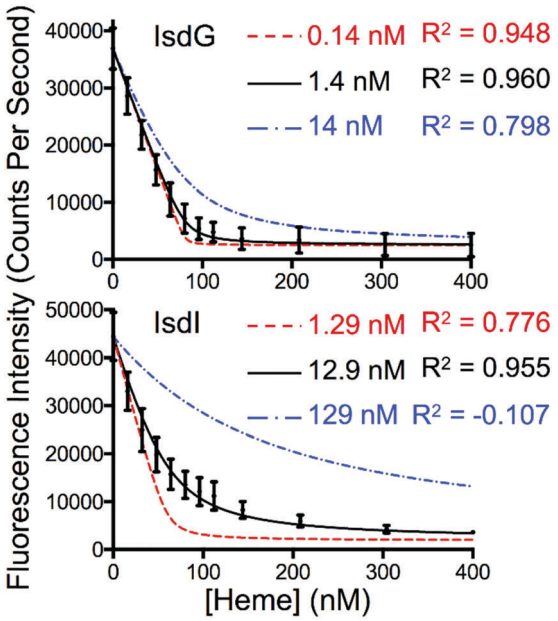

Fig. 6 Best fits of the fluorescence-detected heme titration data for IsdG (top) and IsdI (bottom) using eqn (2) (solid black). The vertical error bars represent the standard deviation of at least three independent measurements. Titration curves predicted using eqn (2) for K_d values one order of magnitude smaller (dotted red) and larger (dashed blue) than the best fit. Based upon the poor fit of the fluorescence-detected heme titration data to K_d values one order of magnitude smaller or larger than the best fit, the K_d values determined by fluorescence spectroscopy are accurate.

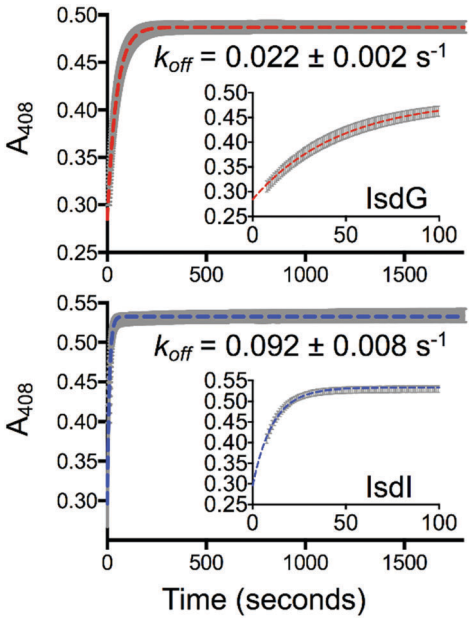

Fig. 7 UV/Vis absorption-detected kinetic traces for heme transfer from 3 μM IsdG–heme to 30 μM apomyoglobin (top) and 3 μM IsdI–heme to 30 μM apomyoglobin (bottom) in 50 mM Tris pH 7.4, 150 mM NaCl. The first 100 s of data are shown in the insets. The gray shaded regions represent the standard deviation of at least three separate measurements. Fits of the kinetic data to eqn (3) yielded k_{off} values of 0.022 ± 0.002 and 0.092 ± 0.008 s^{-1} for IsdG–heme and IsdI–heme, respectively.

Apomyoglobin competition assays

The difference between the K_d values for heme dissociation from IsdG–heme and IsdI–heme suggested that the rates for heme dissociation from IsdG–heme and IsdI–heme may be different. The k_{off} rates for IsdG–heme and IsdI–heme were estimated by measuring the rates of heme transfer to apomyoglobin in a competition assay, an approach that was previously used to estimate k_{off} rates for HO-2,[19] IsdA,[33] IsdB,[34,35] IsdC,[33] and IsdE.[34] Since the K_d for heme dissociation from myoglobin is femtomolar and k_{on} for heme association is on the order of 10^8 M^{-1} s^{-1},[36] these rates will primarily depend upon the k_{off} rates for IsdG–heme and IsdI–heme. Analyses of the kinetic data yielded estimates of 0.022 ± 0.002 and 0.092 ± 0.008 s^{-1} for the k_{off} rates of IsdG–heme and IsdI–heme, respectively (Fig. 7). According to these data, the rate of heme dissociation from IsdG–heme is four-fold slower than heme dissociation from IsdI–heme. This is consistent with the differences between the K_d values reported in this work. As will be discussed below, the heme dissociation differences between IsdG–heme and IsdI–heme have important biological and medical implications.

Discussion

The data reported in this article has important implications for all heme oxygenase enzymes. The nanomolar K_d values measured for IsdG–heme and IsdI–heme are 2–3 orders of magnitude lower than those previously reported for these enzymes.[5] However, the K_d values reported here for IsdG and IsdI are on the same order of magnitude as those recently reported for truncated, soluble forms of HO-1 and HO-2 lending support for the K_d values measured here for non-canonical heme oxygenases.[18,19] The fundamental problem with the older K_d measurements for IsdG and IsdI is that heme is 99.9% protein-bound prior to saturation when a nanomolar dissociation constant is measured at micromolar protein concentrations, which makes accurate curve fitting to extract an accurate K_d value nearly impossible. These data highlight the existence of a dangerous minefield in the biochemical literature. The K_d value for heme dissociation from a heme oxygenase is below the lower limit of detection for UV/Vis absorption spectroscopy, especially if a weak binding approximation is employed. All reported K_d values for HOs must be reviewed on a case-by-case basis, and for cases where micromolar K_d values are accurate, researchers should reconsider whether these proteins are competent heme oxygenases *in vivo*.

Since both IsdG and IsdI are transcriptionally-regulated by the ferric uptake regulator;[3] both degrade heme to non-heme iron,[5] staphylobilin,[6] and formaldehyde;[7] and both are required for pathogenesis in mice; the purpose for two nearly identical enzymes in *S. aureus* has remained an open question. One key clue has been that the half-life of IsdG is increased 2.5-fold by the presence of heme whereas the half-life of IsdI is unaffected by the presence of heme,[3] and now the facts that IsdG and IsdI have different K_d and k_{off} values for heme dissociation can be considered two additional clues. These three facts imply that in low heme conditions, IsdG will be

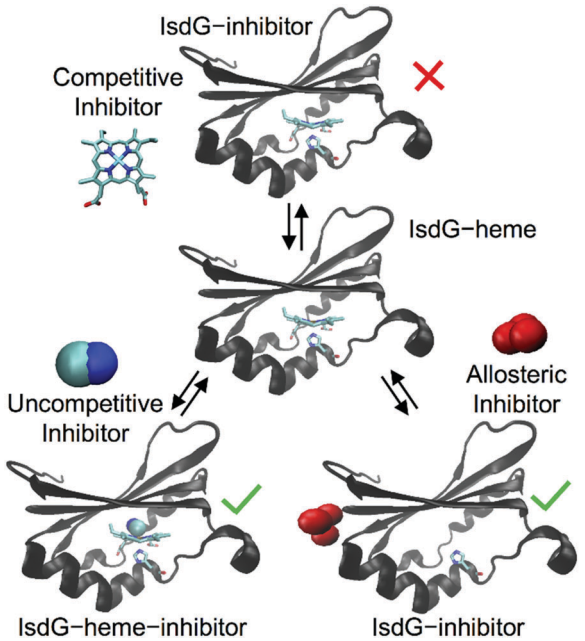

Fig. 8 At least three strategies for IsdG inhibition can be envisaged. Based upon the K_d value reported here, competitive inhibition of IsdG seems impractical. However, uncompetitive or allosteric inhibition of IsdG should be feasible. Due to the significant structural and functional differences between IsdG and mammalian heme oxygenases, elucidation of the IsdG mechanism followed by design of an uncompetitive inhibitor appears to be the most promising strategy for development of a new antibiotic.

degraded and IsdI will be the sole heme oxygenase present at a significant concentration. The K_d value for IsdI is on the same order as the concentration of the cytosolic labile heme pool,[20,21] suggesting that IsdI may regulate heme levels and mitigate heme toxicity.[3] In contrast, when the concentration of cytosolic heme is increased by an active Isd pathway, IsdG will be the primary heme oxygenase due to its lower K_d value. Due to the tight binding of heme by IsdG, there is no apparent need for a heme trafficking protein between the IsdDEF cytoplasmic membrane transporter and IsdG in the *S. aureus* heme iron acquisition pathway.[2,4] Thus, while IsdG and IsdI have the same chemical function, it appears that the two enzymes have distinct biological functions.

Finally, the K_d values reported here have important implications for the rational design of a selective IsdG inhibitor. Since IsdG enzymes have been discovered in several human pathogens, including *S. aureus*,[5] *Bacillus anthracis*,[37] and *Listeria monocytogenes*,[38] they have been identified as potential antibiotic targets.[22,39,40] The first inhibitors of IsdG identified were non-iron metalloporphyrins (Fig. 8),[32] but the tight binding of ferric heme by IsdG now seems to rule out competitive inhibition as a viable strategy. Later, it was established that cyanide and azide are uncompetitive inhibitors of IsdG that bind to the iron of IsdG–heme, block access for molecular oxygen, and prevent enzymatic turnover.[15] Cyanide and azide are poor drugs due to their ability to inhibit canonical heme oxygenases,[41,42] but in principle it should be possible to design a selective, uncompetitive inhibitor for the heme to *meso*-hydroxyheme monooxygenation reaction or the *meso*-hydroxyheme to staphylobilin dioxygenation reaction (Fig. 2).[11,15,16] A third strategy for IsdG inhibition is the development of an allosteric inhibitor analogous to the strategy currently being explored for a canonical heme oxygenase from *Pseudomonas aeruginosa*,[43,44] but there are no promising leads for this strategy and it does not appear necessary due to the significant structural and functional differences between IsdG and canonical heme oxygenases. Thus, the most promising strategy for developing a selective IsdG inhibitor is to elucidate the enzymatic mechanism of IsdG in order to identify and target features of the reaction that are unique compared to canonical heme oxygenases.

Conclusions

In summary, the K_d for heme dissociation from *S. aureus* IsdG and IsdI is 2–3 orders of magnitude lower than previously reported.[5] To be specific, the K_d for heme dissociation from *S. aureus* IsdG is 1.4 ± 0.6 nM and K_d for IsdI is 12.9 ± 1.3 nM. The differences between the current and previous values are attributed to protein concentration; at the micromolar concentrations used previously, heme is 99.9% enzyme-bound making accurate data analysis nearly impossible. Here, the development of a fluorescence spectroscopy-based assay enabled measurements at nanomolar protein concentrations. In addition, apomyoglobin competition assays estimated k_{off} rates of 0.022 ± 0.002 and 0.092 ± 0.008 s^{-1} for IsdG–heme and IsdI–heme, respectively. Notably, these are the first reports of significant differences between the biochemical properties of IsdG and IsdI leading to the proposals that IsdG is the heme degrading member of the *S. aureus* Isd system and IsdI combats heme toxicity. Based upon the tight binding of heme by IsdG, this enzyme is not a good candidate for competitive inhibition. Instead, researchers should pursue uncompetitive inhibition of IsdG, which will be aided by a more detailed understanding of enzyme mechanism.

Acknowledgements

M. D. L. thanks the National Institutes of Health (R01-GM114277) and the National Science Foundation (DMR-1506248) for financial support. In addition, D. P. thanks ACS Project SEED for summer support.

References

1 M. Z. David and R. S. Daum, *Clin. Microbiol. Rev.*, 2010, **23**, 616–687.
2 S. K. Mazmanian, E. P. Skaar, A. H. Gaspar, M. Humayun, P. Gornicki, J. Jelenska, A. Joachmiak, D. M. Missiakas and O. Schneewind, *Science*, 2003, **299**, 906–909.
3 M. L. Reniere and E. P. Skaar, *Mol. Microbiol.*, 2008, **69**, 1304–1315.

4 N. Muryoi, M. T. Tiedemann, M. Pluym, J. Cheung, D. E. Heinrichs and M. J. Stillman, *J. Biol. Chem.*, 2008, **283**, 28125–28136.
5 E. P. Skaar, A. H. Gaspar and O. Schneewind, *J. Biol. Chem.*, 2004, **279**, 436–443.
6 M. L. Reniere, G. N. Ukpabi, S. R. Harry, D. F. Stec, R. Krull, D. W. Wright, B. O. Bachmann, M. E. Murphy and E. P. Skaar, *Mol. Microbiol.*, 2010, **75**, 1529–1538.
7 T. Matsui, S. Nambu, Y. Ono, C. W. Goulding, K. Tsumoto and M. Ikeda-Saito, *Biochemistry*, 2013, **52**, 3025–3027.
8 C. A. Wakeman, D. L. Stauff, Y. Zhang and E. P. Skaar, *J. Bacteriol.*, 2014, **196**, 1335–1342.
9 R. Tenhunen, H. S. Marver and R. Schmid, *J. Biol. Chem.*, 1969, **244**, 6388–6394.
10 Y. Liu, P. Moënne-Loccoz, T. M. Loehr and P. R. Ortiz de Montellano, *J. Biol. Chem.*, 1997, **272**, 6909–6917.
11 B. R. Streit, R. Kant, M. Tokmina-Lukaszewska, A. I. Celis, M. M. Machovina, E. P. Skaar, B. Bothner and J. L. DuBois, *J. Biol. Chem.*, 2016, **291**, 862–871.
12 R. T. Syvitski, Y. Li, K. Auclair, P. R. Ortiz de Montellano and G. N. La Mar, *J. Am. Chem. Soc.*, 2002, **124**, 14296–14297.
13 R. Garcia-Serres, R. M. Davydov, T. Matsui, M. Ikeda-Saito, B. M. Hoffman and B. H. Huynh, *J. Am. Chem. Soc.*, 2007, **129**, 1402–1412.
14 H. Chen, Y. Moreau, E. Derat and S. Shaik, *J. Am. Chem. Soc.*, 2008, **130**, 1953–1965.
15 C. L. Lockhart, M. A. Conger, D. Pittman and M. D. Liptak, *J. Biol. Inorg. Chem.*, 2015, **20**, 757–770.
16 S. J. Takayama, S. A. Loutet, A. G. Mauk and M. E. Murphy, *Biochemistry*, 2015, **54**, 2613–2621.
17 S. Sano, T. Sano, I. Morishima, Y. Shiro and Y. Maeda, *Proc. Natl. Acad. Sci. U. S. A.*, 1986, **83**, 531–535.
18 S. Koga, S. Yoshihara, H. Bando, K. Yamasaki, Y. Higashimoto, M. Noguchi, S. Sueda, H. Komatsu and H. Sakamoto, *Anal. Biochem.*, 2013, **433**, 2–9.
19 A. S. Fleischhacker, A. Sharma, M. Choi, A. M. Spencer, I. Bagai, B. M. Hoffman and S. W. Ragsdale, *Biochemistry*, 2015, **54**, 2709–2718.
20 Y. Song, M. Yang, S. V. Wegner, J. Zhao, R. Zhu, Y. Wu, C. He and P. R. Chen, *ACS Chem. Biol.*, 2015, **10**, 1610–1615.
21 D. A. Hanna, R. M. Harvey, O. Martinez-Guzman, X. Yuan, B. Chandrasekharan, G. Raju, F. W. Outten, I. Hamza and A. R. Reddi, *Proc. Natl. Acad. Sci. U. S. A.*, 2016, **113**, 7539–7544.
22 S. A. Loutet, M. J. Kobylarz, C. H. T. Chau and M. E. P. Murphy, *J. Biol. Chem.*, 2013, **288**, 25749–25759.
23 L. Yi and S. W. Ragsdale, *J. Biol. Chem.*, 2007, **282**, 21056–21067.
24 A. B. Graves, E. H. Horak and M. D. Liptak, *Dalton Trans.*, 2016, **45**, 10058–10067.
25 R. B. Kapust, J. Tözsér, J. D. Fox, D. E. Anderson, S. Cherry, T. D. Copeland and D. S. Waugh, *Protein Eng.*, 2001, **14**, 993–1000.
26 F. W. J. Teale, *Biochim. Biophys. Acta*, 1959, **35**, 543.
27 E. L. Carter, N. Gupta and S. W. Ragsdale, *J. Biol. Chem.*, 2016, **291**, 2196–2222.
28 E. A. Berry and B. L. Trumpower, *Anal. Biochem.*, 1987, **161**, 1–15.
29 A. B. Graves, R. P. Morse, A. Chao, A. Iniguez, C. W. Goulding and M. D. Liptak, *Inorg. Chem.*, 2014, **53**, 5931–5940.
30 M. S. Hargrove, E. W. Singleton, M. L. Quillin, L. A. Ortiz, G. N. Phillips and J. S. Olson, *J. Biol. Chem.*, 1994, **269**, 4207–4214.
31 R. M. C. Dawson, C. D. Elliot, W. H. Elliot and M. K. Jones, *Data for Biochemical Research*, Clarendon Press, Oxford, UK, 1989.
32 W. C. Lee, M. L. Reniere, E. P. Skaar and M. E. P. Murphy, *J. Biol. Chem.*, 2008, **283**, 30957–30963.
33 M. Liu, W. N. Tanaka, H. Zhu, G. Xie, D. M. Dooley and B. Lei, *J. Biol. Chem.*, 2008, **283**, 6668–6676.
34 H. Zhu, G. Xie, M. Liu, J. S. Olson, M. Fabian, D. M. Dooley and B. Lei, *J. Biol. Chem.*, 2008, **283**, 18450–18460.
35 C. F. M. Gaudin, J. C. Grigg, A. L. Arrieta and M. E. Murphy, *Biochemistry*, 2011, **50**, 5443–5452.
36 M. S. Hargrove, D. Barrick and J. S. Olson, *Biochemistry*, 1996, **35**, 11293–11299.
37 E. P. Skaar, A. H. Gaspar and O. Schneewind, *J. Bacteriol.*, 2006, **188**, 1071–1080.
38 T. Duong, K. Park, T. Kim, S. W. Kang, M. J. Hahn, H.-Y. Hwang and K. K. Kim, *Acta Crystallogr., Sect. D: Biol. Crystallogr.*, 2014, **70**, 615–626.
39 A. Wilks and K. A. Burkhard, *Nat. Prod. Rep.*, 2007, **24**, 511–522.
40 J. E. Choby and E. P. Skaar, *J. Mol. Biol.*, 2016, **428**, 3408–3428.
41 G. Hernandez, A. Wilks, R. Paolesse, K. M. Smith, P. R. Ortiz de Montellano and G. N. La Mar, *Biochemistry*, 1994, **33**, 6631–6641.
42 Y. Zeng, G. A. Caignan, R. A. Bunce, J. C. Rodríguez, A. Wilks and M. Rivera, *J. Am. Chem. Soc.*, 2005, **127**, 9794–9807.
43 K. Hom, G. A. Heinzl, S. Eakanunkul, P. E. M. Lopes, F. Xue, A. D. MacKerrell and A. Wilks, *J. Med. Chem.*, 2013, **56**, 2097–2109.
44 G. A. Heinzl, W. Huang, W. Yu, B. J. Giardina, Y. Zhou, A. D. MacKerrell, A. Wilks and F. Xue, *J. Med. Chem.*, 2016, **59**, 6929–6942.